Seismicity of the New Madrid Seismic Zone Derived from a Deep-Seated Strike-Slip Fault

by Behrooz Tavakoli, Shahram Pezeshk, and Randel Tom Cox

Abstract   A conceptual three-dimensional flower structure model of strike-slip faulting is proposed to explain the occurrence of earthquakes in the New Madrid seismic zone (NMSZ) and to illustrate the potential rupture faults for the 1811–1812 earthquake sequences. The proposed NMSZ model is based on elastic dislocation theory and concepts of material failure under a stress field. Using a conceptual model of a strike-slip subsidiary fault array, we identify tectonic features (geological structures) that are oriented properly relative to regional stresses and classify the regions where stresses might be expected to be amplified.

The brittle upper crust in the vicinity of the NMSZ is modeled as a uniform overburden with a horizontal-basal surface, which rests on a horizontal ductile lower crust that is cut by a vertical, northeast-striking right-lateral strike-slip shear zone. We acknowledge that many favorably oriented preexisting faults have been exploited as components of the flower structure. The brittle overburden material is subject to simple shearing stress parallel to the deep-seated lower crustal shear zone, and preexisting faults of the Reelfoot rift system give the upper crust a mechanical anisotropy (planes of weakness striking northeast) that is the correct orientation for development of P shear faults. The deep-seated fault movement deforms the overlying upper crust that controls the structural geometry, the modern seismicity, and the large earthquake sequences in the NMSZ.

The three-dimensional NMSZ model of faulting developed in this study shows that the Bootheel and Big Creek lineaments, inferred to be two subparallel P shear faults rooted in a deep-seated fault in the lower crust, are significant in shaping the geometry of the NMSZ. These series of faults produce a large-scale flower structure in cross section. The proposed NMSZ model uses the intersections of the deep-seated fault and the two subparallel P shear faults for the locations of the 1811 and 1812 earthquakes. The model gives rise to a predictable pattern of surface deformation that is in good agreement with the observed seismicity patterns in the region.

Introduction

Understanding the mechanics of tectonic faulting that generates seismicity patterns in intraplate regions such as the New Madrid seismic zone (NMSZ) has long been an outstanding geodynamic problem. Four large earthquakes with magnitudes **M** 7.0–8.0 occurred during the winter of 1811–1812 within the NMSZ (Johnston, 1996; Hough and Martin, 2002; Bakun and Hopper, 2004). There is, however, no single mechanical explanation that has been widely accepted to account for the occurrence of earthquakes along the faults in the region. Identifying and characterizing geological structures that could generate earthquakes in the NMSZ is an important step in seismic hazard evaluations. We propose a new working hypothesis that NMSZ faulting is an array of subsidiary faults expected for a right-lateral shear zone in the

lower crust. We infer that the four largest earthquakes of the 1811–1812 New Madrid sequence may have occurred along a deep-seated fault triggering the thrust rupture on the Reelfoot fault.

Many researchers have proposed that seismicity in the New Madrid region is concentrated in a zone of crustal weakness (Sykes, 1978; Braile *et al.*, 1986; Cox and Van Arsdale, 1997; Csontos *et al.*, 2008). According to crustal weakness models, the current seismicity of the NMSZ is due to reactivation of ancient rift-originated faults, but these models do not explain the recurrence of the large-magnitude earthquakes in the region. In addition, Liu and Zoback (1997) have shown that temperatures in the lower crust of the NMSZ appear to be high relative to surrounding areas. Kenner and Segall

(2000) have proposed a time-dependent mechanical NMSZ model for the generation of the large earthquakes defining a weak lower crustal zone within an elastic lithosphere. This weak zone transfers stress to the upper crust and may trigger slip on overlying faults, generating a sequence of earthquakes. Although the source of stress buildup is in the lower crust, this model does not clarify the pattern of seismicity and surface features in the NMSZ. Schweig and Ellis (1994) have argued that the NMSZ has experienced a rotation of stress field within the last three million years. They have presented a simple tectonic model based on the geology and seismicity of the NMSZ showing a fault system as a left-stepping, right-lateral strike-slip fault system. Gomberg and Ellis (1994) have analyzed this fault system to test hypothetical mechanisms that constrain the three-dimensional deformation in the NMSZ. They have suggested that the observed deformation in the NMSZ appears to require slip both on two southwest dipping faults in the left-stepover region and on two northeast-trending vertical, right-lateral faults.

Fault segmentation provides a physical framework to determine both the size and potential location of future earthquakes on a fault zone (Scholz, 1990). Johnston and Schweig (1996) have identified the causative-fault segments for the large historical earthquakes in the NMSZ solely from microseismicity and physical constraints. However, neotectonic studies within the NMSZ (Nelson et al., 1997; Cox, Van Arsdale, and Harris, 2001) show that the large earthquakes may occur on faults not characterized by frequent small seismic events. These active structures that are unrecognizable through current seismicity may be the source of the next large earthquakes in the region.

Explaining seismicity by hypothesizing localized sources of stress is inconsistent with the observation that relatively uniform stress fields seem to characterize seismic areas and the surrounding regions. Zoback and Zoback (1981) have inferred that the orientations of the principal axis of compressional stress in the region surrounding the NMSZ is horizontal and about N80°E, in agreement with suggested focal mechanism solutions (Herrmann, 1979; Ellis, 1994). Although there is a relatively uniform regional stress field throughout the NMSZ, one may question why the tectonic stress field gives rise to the branching seismicity pattern of the NMSZ.

The objective of the present paper is to present a new model of NMSZ faulting to explain the odd fault geometry using an analog model of subsidiary structures associated with a deep-seated strike-slip fault (Tchalenko and Ambraseys, 1970; Wilcox et al., 1973). A left-stepover en echelon right-lateral strike-slip fault model has been suggested based on the fault patterns inferred from the seismicity (Russ, 1982). In the 1982 Russ's model, some component of the shear strain in the left-stepover region is accommodated by right-lateral slip on the northeast-trending seismic zone along the axis of the Reelfoot rift. We modify this model to incorporate synthetic (*P* shears) and antithetic (Riedel *R* shears) of an upward splaying strike-slip shear zone rooted in the lower crust. The

present study predicts faults and subsurface structures, some of which spatially correlate with specific trends in modern seismicity. This three-dimensional model of NMSZ deformation is used to determine the dimensions of possible seismic source zones and the mechanics of tectonic faulting, which might develop in the region over time. We discuss the ways to incorporate a new possible earthquake rupture scenario into the seismic hazard analysis of the NMSZ describing the presence of intersecting tectonic features and illustrating how the three-dimensional model of NMSZ deformation (as developed in this study) affects fault behavior during the 1811–1812 earthquake sequence.

Geologic and Seismotectonic Setting of the NMSZ

The NMSZ is the most seismically active area in the central and eastern United States. Most of the modern seismicity of the NMSZ occurs within the geographical limit of the Reelfoot rift, and a well-known linear zone of seismicity coincides with the axis of the rift (Fig. 1). The Reelfoot rift (which is interpreted from geophysical data) is a northeast-trending, 300 km long, 70 km wide graben with a structural relief of ∼2 km between the interior of the graben and the surrounding basement (Hildenbrand et al., 1992; Van Arsdale et al., 1998; Csontos et al., 2008). Although there is surface evidence for late Quaternary right-lateral strike-slip movement on the Reelfoot margins, net fault separation in the basement is dip slip (Chiu et al., 1997; Cox, Van Arsdale, Harris, and Larsen, 2001).

An understanding of the regional seismotectonic history and identification of near-surface deformation are important in determining the potential for damaging earthquakes along and within the rift margins. Since 1974, an extensive network of seismographs has recorded earthquakes in the NMSZ and created an adequate database to use as a basis for understanding the local seismicity. As shown in Figure 1, the distribution of earthquakes indicates four major trends of seismicity in the region (Stauder, 1982; Himes et al., 1988; Johnson, 2008). The northeast-trending seismic zone (Z1) intersects a broader, northwest-trending zone of more intense activity (Z2). Seismicity continues to the northeast along the northwestern margin of the Reelfoot rift near New Madrid, Missouri (Z3). Seismicity along the northeast trend from Marked Tree to Caruthersville (Z1) occurs in near-vertical fault zones at depths of 5–15 km and focal mechanisms indicate right-lateral slip (Chiu et al., 1992). In the northwest-trending zone from New Madrid to Dyersburg (Z2), the earthquakes occur at similar depths but along planes that dip at 32°–55° (Csontos and Van Arsdale, 2008) toward the southwest and exhibit mainly strike slip and thrust motion (Chiu et al., 1992). The northeast-trending zone of earthquakes from New Madrid to Charleston (Z3) may be related to sets of near-vertical, right-lateral faults (Johnson, 2008). In general, the central segment (Z2) seems to represent a left-restraining step connecting the two right-lateral strike-slip fault segments (Russ, 1982). The large earthquakes of
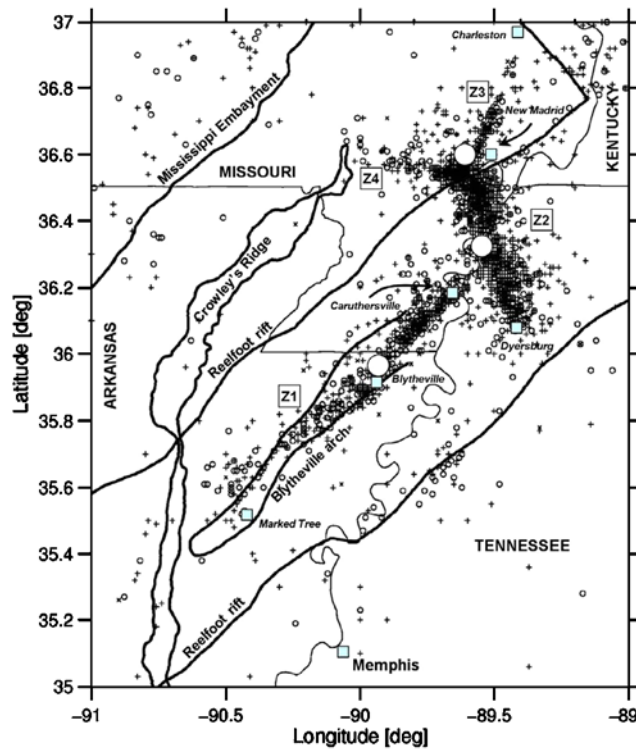
Figure 1. Location of historical earthquakes with $M \geq 2.0$ in the NMSZ for the period of 1974–2008. A cross represents an event at the depth of 10 km or shallower, and a small circle represents an event at the depth of between about 10 and 20 km. The open circles show the locations of the largest earthquakes of 1811–1812 in relation to the axis of the Reelfoot rift and the Blytheville arch in the Mississippi embayment. The earthquake data recorded by the New Madrid seismograph network, the catalog of eastern North American earthquakes compiled by Seeber and Armbruster (1991), and the historical earthquakes compiled by Johnston and Schweig (1996) are considered in this study. The small boxes show the locations of the major cities within the Mississippi embayment. Z1, Z2, Z3, and Z4 denote the principal seismicity alignments. The color version of this figure is available only in the electronic edition.

1811–1812 are believed to have been located in the region between Marked Tree and Blytheville, Arkansas, and the area near New Madrid (Nuttli, 1973; Hamilton and Johnston, 1990; Bakun and Hopper, 2004). The fourth seismic zone (Z4) to the west of the town of New Madrid trends westnorthwest and is much shorter than the other three major segments mentioned previously. Focal mechanism solutions for events along this fault segment indicate left-lateral slip on a near-vertical plane (Chiu *et al.*, 1992; Johnson, 2008).

Inferred structures along the linear active zones of seismicity have been imaged by seismic reflection (Zoback *et al.*, 1980; Hamilton and Zoback, 1982; Mooney *et al.*, 1983; Howe, 1985; Hamilton and McKeown, 1988; McKeown *et al.*, 1990). In the Reelfoot rift between Marked Tree, Arkansas, and Caruthersville, Missouri, the major trend of modern seismicity coincides with the Blytheville arch (Fig. 1). The vast majority of small earthquakes along the arch are confined to the area of intense arch-related deformation. The Blytheville

arch is divided into two parts: a northeasterly part between the towns of Blytheville and Caruthersville corresponding with a northeast extension called the Cottonwood Grove fault (CGF) (Fig. 2) and a southwesterly part from Blytheville to the end of the feature at Crowley's Ridge (Hamilton and McKeown, 1988) called the Blytheville fault (BVF). Crowley's Ridge is a 320 km long topographic ridge that overlies and crosses the western margin of Reelfoot rift (Fig 1).

Figure 2 illustrates a new simple tectonic model of the possible active faults in the NMSZ based on subsurface data that coincide with the regional distribution of earthquakes or exceptionally strong lineaments from aerial photos and a conceptual model of subsidiary structures associated with a deepseated strike-slip fault. In this study, the tectonic model of the NMSZ is characterized by two large-scale subparallel faults that are rooted in deep-seated faulting in the basement.

The first large-scale subparallel fault, which has been mapped from Charleston, Missouri, to the town of Marked Tree, Arkansas, consists of two principal segments, namely
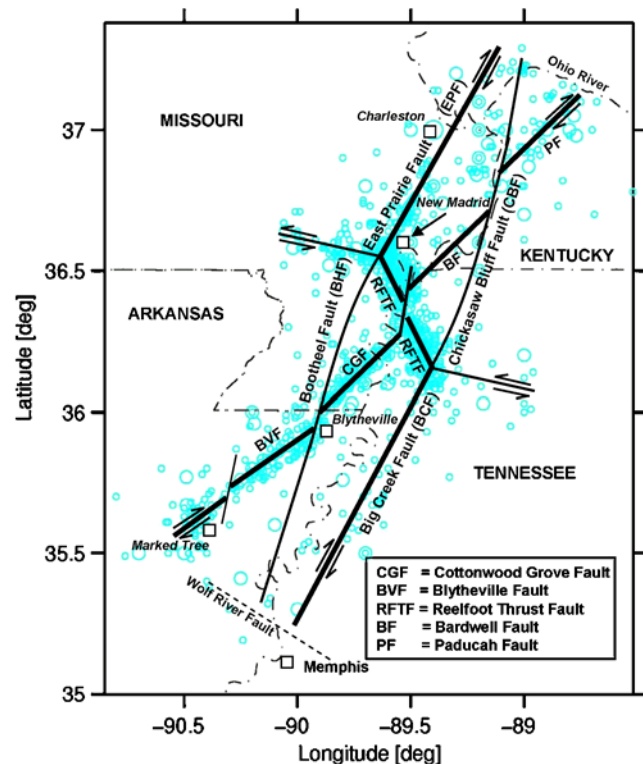
Figure 2. The principal faults considered in the development of a conceptual model of faulting for causing earthquakes in the NMSZ. The locations are based on the earthquakes in the catalogs, on subsurface geophysical data, and on aerial photos. The proposed segment boundaries may represent complex transition zones ranging from a few to more than 70 km across. The boundaries selected on the basis of microseismicity, geometry, and geomorphic observations are coincident with faults and structural trends interpreted from seismic reflection data and geodetic changes. BVF, Blytheville fault; CGF, Cottonwood Grove fault; BF, Bardwell fault; PF, Paducah fault. The color version of this figure is available only in the electronic edition.

the Bootheel fault (BHF) and the East Prairie fault (EPF) (Fig. 2). The BHF, extending north-northeastward from east of Marked Tree, Arkansas, to west of New Madrid, Missouri (Schweig and Marple, 1991), does not coincide with any of the major trends in seismicity but intersects the southwestern part of the CGF at a low angle near Blytheville, Arkansas (Schweig *et al.*, 1992). The strike of the faults and the regional stress directions in the region imply a right-lateral strike-slip movement on the BHF (Schweig and Marple, 1991) and the EPF (Chiu *et al.*, 1992) segments, and a 2.4 k.y. old Holocene paleochannel is dextrally displaced at least 13 m (Guccione *et al.*, 2005).

The Big Creek fault (BCF) is the second large-scale subparallel fault that may be related to a deep-seated fault in the lower crust. The BCF extends north-northeastward along the bluffs east of the Mississippi River and continues as the Chickasaw Bluff fault (CBF). The New Madrid earthquakes of 1811–1812 reportedly triggered many landslides along more than 200 km of bluffs forming the eastern edge of the Mississippi alluvial plain between Cairo, Illinois, and Memphis, Tennessee (Jibson and Keefer, 1992).

Global Positioning System vectors reported for stations on either side of the BCF (Newman *et al.*, 1999; Gan and Prescott, 2001; Smalley *et al.*, 2005) indicate that the region west of the BCF is moving northeastward relative to the region east of the fault zone. Thus, the BCF may be a principal active structure of the southeastern Reelfoot rift margin that is accommodating much of the right-lateral strain in the upper Mississippi embayment (Cox, Van Arsdale, and Harris, 2001). We believe that the BHF/EPF and BCF/CBF right-lateral strike-slip fault zones are interacting across an ~72 km compressional zone along the Reelfoot thrust fault (RFTF). This area is mostly characterized by complex compressional structures including thrusts, folds, conjugate strike-slip faults, and uplift between the two subparallel faults. The restraining left stepover is the geometric discontinuity that causes difficulty for right-lateral motion along strike-slip faults. Theoretical models of faulting (Rodgers, 1980; Segall and Pollard, 1980) indicate that discontinuities between two subparallel faults play an important role in the surface deformation and the prediction of secondary fault systems.

The subparallel BHF/EPF and BCF/CBF faults are rooted in the lower crust and join together into a northeast-striking, vertical fault zone at depth, herein called the deep-seated New Madrid fault. The New Madrid fault beneath the seismic zone is speculated to be a more ductile zone due to heating by magma intrusion occurring 90 m.y.a. along the preexisting 0.5 billion year old Reelfoot rift faults (Hildenbrand *et al.*, 1982). Currently this fault is being sheared due to horizontal compression of the westward-moving North America plate. In the brittle upper crust, as shown in Figure 2, the deep-seated fault has several left-stepping en echelon fault segments (e.g., BVF, CGF, BF, and PF). The Bardwell fault (BF) and the Paducah fault (PF) are proposed herein. These series of segmented and subparallel faults produce flower structures on many scales.

We consider a conceptual model of subsidiary strike-slip faulting for the NMSZ region based on both theoretical and experimental considerations and use this working hypothesis to interpret the spatial pattern of seismicity, the relationship among faults, and the tectonic stress field in the NMSZ.

A Conceptual Kinematic Model of Faulting in the NMSZ

In most experimental and observational studies, strike-slip faults derived from displacements along deep-seated faulting in the basement generally display an en echelon pattern of subsidiary faults (Tchalenko, 1970). In the en echelon pattern, the strike-slip faults often consist of a series of synthetic strike-slip faults (having the same sense of movement as the principal shear plane), antithetic strike-slip faults (having the opposite sense), normal faults, and reverse faults (Fig. 3). Synthetic faults include Riedel (*R*) and *P* shear faults, and antithetic faults are conjugate Riedel (*R′*) faults. Wilcox *et al.* (1973) suggested that internal rotation of the en echelon strike-slip faults is caused by compressive deformation not related to deep-seated faulting. Fault rotation occurs where material is subjected to the external shear stress that acts perpendicular to the direction of the major shear displacement (Ramsey, 1980). One may easily verify that a similar result can be obtained by the Coulomb–Mohr theory of failure. The right-lateral shear faults have clockwise external rotation. Areas that undergo these conditions (Fig. 3) can develop Riedel *R* and *P* shear faults (Tchalenko and Ambraseys, 1970).

If the strike-slip movement takes place at sufficient depth, then normal faults may develop en echelon in the cover above the displaced blocks but still under considerable lithostatic pressure, which guarantees that the maximum stress is vertical (Fig. 3). Where the principal strike-slip fault movement is not confined to a narrow zone, subsidiary normal faults frequently combine to form horst or graben. Normal faulting may develop over a wide area with only a very loose directional relationship to the deep-seated fault movement.

We consider strike-slip fault systems in the NMSZ, dealing sequentially with primary, subsidiary synthetic, and subsidiary antithetic systems. When the crust of the NMSZ is subjected to a sufficiently high horizontal compression (σ_1), a primary strike-slip fault (deep-seated fault) develops within a certain depth range where the intermediate principal stress (σ_2) is vertical. This is the Master fault or Y-shear in Figure 3, and the deep-seated fault in Figure 4. Figure 4a shows two boxes inscribed across a strike-slip fault that become separated by motion on the deep-seated fault and also deformed into parallelograms by shearing distributed on either side of the fault. The right-lateral strike-slip movement along the deep-seated fault generates a secondary stress system in which the maximum horizontal compression (σ_1) assumes a position oblique to the vectors of force couple in the basement. Subsidiary strike-slip faults are thus developed obliquely to the primary strike-slip movement (Fig. 4a). The development of Riedel *R* shears has been inhibited because
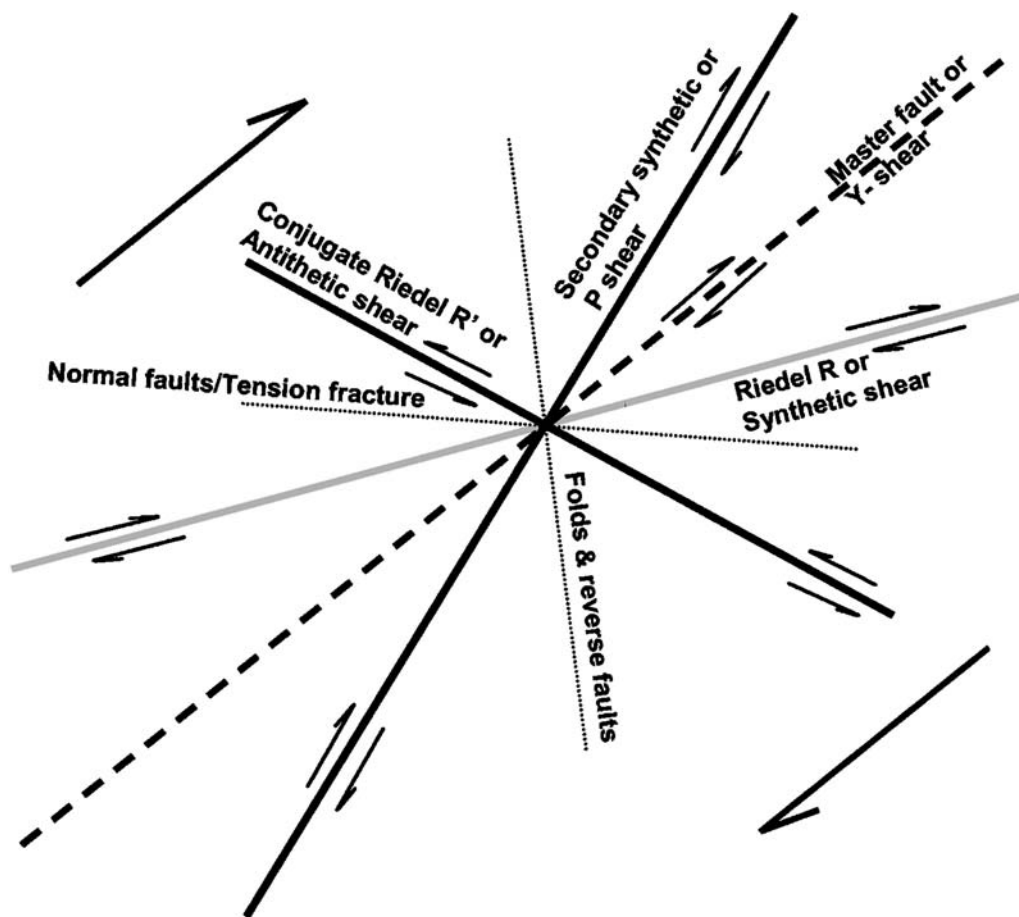
Figure 3.   Idealized right-lateral simple shear, compiled from clay models and from geological observations. Fractures and folds are superimposed on a strain model for the overall deformation and terminology of structures.

strain above the deep-seated fault has been largely accommodated by slip on preexisting faults of the upper crustal Reelfoot rift system that reactivated as synthetic P shears. The senses of movement along the subsidiary P shear faults can be readily predicted from their positions relative to the stress system. Synthetic P shear faults form at a low angle to the primary fault (e.g., BHF/EPF and BCF/CBF segments) and have the same sense of displacement as that of the deep-seated faulting (right-lateral strike-slip movement).

In contrast, antithetic shear faults (R' in Fig. 4a) have a displacement sense opposite that of the deep-seated faulting (left-lateral strike-slip movement) and form at a high angle to it. The acute angle of intersection of the synthetic and antithetic shear faults is dependent on the properties of the rocks and the deformation. This angle is bisected by the direction of maximum horizontal compression. Synthetic subsidiary faults typically form in an en echelon series above the primary strike-slip fault, and there is commonly overlap between the ends of consecutive synthetic shear faults (Fig. 4b).

The overlap of synthetic P shear faults we assume in this study (BHF/EPF and BCF/CBF) contains the RFTF in the NMSZ. Movement along these right-lateral strike-slip faults causes the material to be compressed in the region of overlap.

This causes an increase in the magnitude of maximum horizontal stress (σ_1) and, in turn, develops both typical uplifts with boundary thrust faults (Fig. 4b) and new synthetic strike-slip faults (R in Fig. 4c). These restraining bend faults are restricted to the neighborhood of fault tips where a stress concentration occurs. The sense of slip along these faults depends mainly on the reorientation of principal stress trajectories and on the changed shear stress distribution. This simplified kinematic model of a strike-slip fault system is discussed here to gain insight into the complexities that can develop in the NMSZ.

Surface Expressions of Deep-Seated New Madrid Fault

According to the NMSZ model of deformation developed in this study, the upper ~15 km of the crust in the vicinity of the NMSZ is modeled as a uniform brittle overburden, which rests on a horizontal ductile lower crust that is intersected by a vertical shear zone. A vertical northeast-striking lower crustal shear zone beneath the NMSZ might be present due to a residual zone of elevated temperature in the lower crust due to magma intrusion along the Reelfoot rift
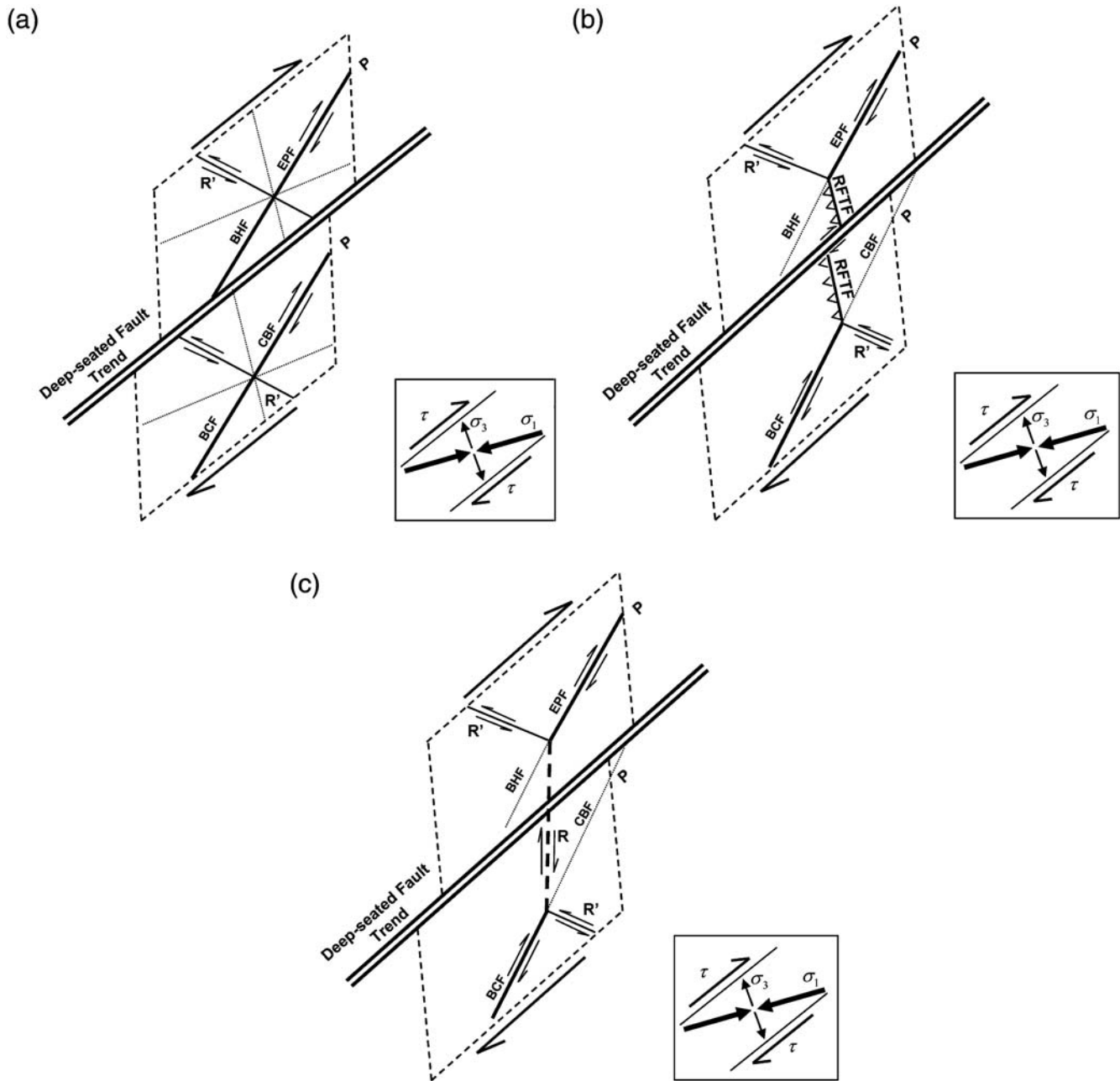
Figure 4. The conceptual kinematic model of faulting when the crust of the NMSZ is subjected to a sufficiently high horizontal compression (σ_1). (a) The orientation of failure surfaces is formed by the action of a force couple and reactivation of preexisting faults favorably oriented for subsidiary faults to the deep-seated fault. (b) The movement of derivative subparallel faults and deep-seated fault causes the material to be compressed in the region of overlap (RFTF). The kinematic model shows that the left stepover occurs in the right-lateral fault zones (deep-seated fault and two subparallel *P* shear faults). (c) The large stress in the compression zone will develop a new Riedel (*R*) shear fault to connect the subparallel *P* shear faults. The regional stress field encourages right-lateral movement on the subparallel *P* shear faults and left-lateral movement on conjugate Riedel (*R′*) shear faults. BHF, Bootheel fault; EPF, East Prairie fault; BCF, Big Creek fault; CBF, Chickasaw Bluff fault; RFTF, Reelfoot thrust fault.

faults about 90 m.y.a. (Cox and Van Arsdale, 2002). Such a residual thermal zone has been argued for 115–140 Ma intrusions in Quebec (Eaton and Frederiksen, 2007).

The brittle overburden material above the basement fault is subject to simple shearing parallel to the basement fault when the basement is displaced along this fault in purely horizontal relative movement. Zoback (1992) suggests that

stresses in the NMSZ are probably related to drag forces at the base of the North America plate. Zoback (1992) infers that the orientation of the force couple under simple shear condition will be ≈N42°E, which is coincident with the axis of the Reelfoot rift within the Mississippi embayment. The three-dimensional geometry of individual shear faults within an overburden above deep-seated strike-slip faulting with the

angle of view from southwest to northeast is shown schematically in Figure 5.

It should be noted that the overburden at some lateral distance from the basement fault is passively dragged by the basement faulting and that the horizontal shear stress imposed by the faulting decreases upward and vanishes at the Earth's surface. Hence, in the shallow parts of the upper crust the material may be considered under simple shear, imposed by the outer parts of the brittle crust. This further implies that close to the horizontal surface between the lower and upper crust, two principal stress directions are parallel to the surface, which has a profound influence on the development of subsurface structures. The near-surface faults are generated by pure right-lateral strike slip along a single basement fault (Fig. 5).

The deep-seated New Madrid fault is coincident with the northeast-trending zone of seismicity and the Blytheville arch in the NMSZ. Focal mechanisms of earthquakes in this zone are indicative of right-lateral strike-slip faulting on vertical, northeast-trending planes. We speculate that the lower crustal shear zone has taken advantage of the most favorably

oriented preexisting upper crustal Reelfoot rift faults to approximate a subsidiary fault array, and in this setting, preexisting faults were suitably oriented for *P* shears but not for *R* shears. The BHF/EPF and the BCF/CBF are behaving as *P* shears and appear to be significant in shaping the topography, geologic structure, and seismicity pattern of the NMSZ. These features are used to infer the strike, length, width, and type of faulting for the subordinate faults derived from a basement fault in the region. The helicoidal shape of the linked faults that comprise the BHF/EPF and BCF/CBF systems (Fig. 5) is required by the reorientation of the principal stresses, which is caused by the shear stresses imposed on the overburden by the movement along the basement fault (Mandl, 1988). Locations where faults intersect are the concentration of stresses and in turn the areas of the greater fracture density for the nucleation of the intermediate and large earthquakes.

The direction of concentrated strike-slip movement at depth need not necessarily coincide with the axis of the en echelon series at the surface, but the deviation is quite small and mostly affects the outer parts of the strike-slip
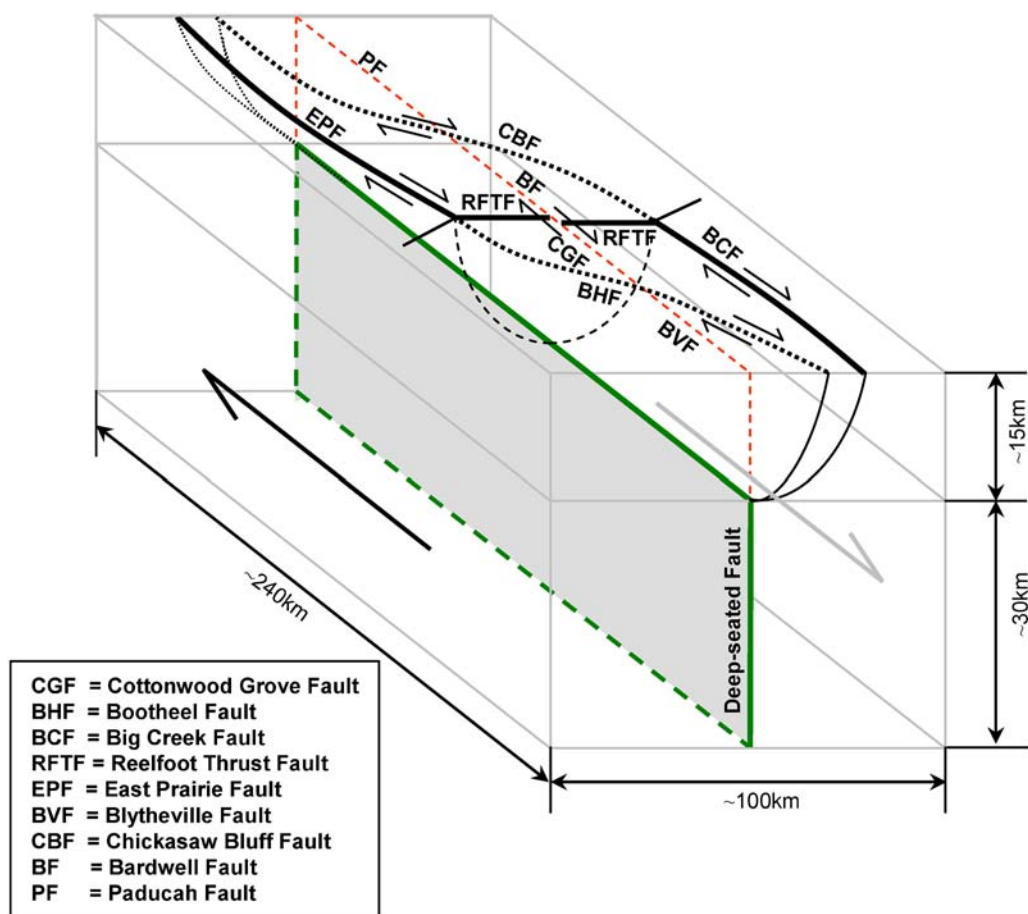
Figure 5.   Sketch of three-dimensional model of faulting in the NMSZ. Stress concentration on subparallel faults in upper crust is generated by pure strike slip of a deep-seated fault in the right-lateral sense. The subparallel faults are concave in vertical sections perpendicular to the strike of the deep-seated fault (helicoidal shape). This fault geometry causes the material in the upper crust to be squeezed upward in the uplift region (RFTF) between shear faults. Uplift decreases with depth to zero where the subsidiary joins the deep-seated fault. The color version of this figure is available only in the electronic edition.

zone. As indicated in Figure 5, right-lateral deep-seated strike-slip faulting will cause compressional overburden structures between two adjacent shear faults in the region of overlap. The material tends to be squeezed upward in the region between two shear faults where the strike-slip motion is obstructed most. This uplift diminishes with depth to zero at the lower crustal shear zone. When the principal strike-slip movement occurs at shallow levels, reverse faults are liable to develop rather than normal faults at 90° to the σ_1 trajectories.

At shallow depths, complex fault interactions may give rise to subsidiary oblique-slip faults, such as are frequently observed in the shallow uplift zone of New Madrid. Uplift between the *P* shear faults (BHF/EPF and BCF/CBF) has been mapped at the surface for ~32 km southeast of New Madrid and continues ~40 km as a subtle warp to near Dyersburg, Tennessee, for a total length of ~72 km (Van Arsdale et al., 1995, 1999). According to the three-dimensional NMSZ model of deformation developed in this study, surface motion around the RFTF partitions into several blocks. The uplift of ~10 m for the northwest block in the Lake County uplift (Russ, 1982) and an increase of ~2 m in the height of Reelfoot scarp at the time of the 1811–1812 events (Kelson et al., 1996) and ~1 m of subsidence in the Reelfoot Lake basin can be interpreted as indicative of relative tectonic between blocks.

The conceptual NMSZ model developed in this study assumes that the magnitudes of the stresses associated with faults are insufficient for second-order faults and other second-order structures to develop along the walls of the principal fault and that second-order structures can develop only at the extremes of the principal fault or principal uplift axes, where a stress concentration occurs. This may result in the formation of splay faults that are subsidiary strike-slip faults. The analysis of focal mechanisms for the events along the major trends of seismicity in the NMSZ (Herrmann and Canas, 1978; Chiu et al., 1992; Johnson, 2008) and our conceptual NMSZ model of faulting confirms that the Z3 branch shown in Figure 1 is right-lateral *P* shear fault while the western branch (Z4) is left-lateral antithetic shear fault (conjugate Riedel *R'* in Fig. 3).

Besides the Z4 branch shown in Figure 1, which is called northern left-lateral fault (NLF) in Figure 6, the conceptual NMSZ model of faulting also indicates a possible left-lateral strike-slip fault near Dyersburg that we have herein called the eastern left-lateral fault (ELF). The ELF may be considered as a part of the rupture sequence to generate large earthquakes in the NMSZ. For example, right-lateral strike-slip movement on the BCF and left-lateral movement on the ELF would confine an area of enhanced stress near the intersection (tip zone). This tip zone, located near Dyersburg, would be able to generate large earthquakes over time (Fig. 6).

Geological Controls on the Seismogenic Faults

The three-dimensional conceptual model of faulting in NMSZ developed in this study argues that the local seismicity

of the NMSZ correlates with a master deep-seated strike-slip fault parallel to the axis of the Reelfoot rift (the New Madrid fault). The northeast strike of Reelfoot rift combined with the known east-northeast orientation of maximum regional compression allows us to consider a vertical, right-lateral movement for the deep-seated fault. A secondary set of fault zones strike northwest in the basement and interacts with the New Madrid fault (Hildenbrand et al., 1992; Cox, Van Arsdale, and Harris, 2001; Csontos et al., 2008).

We assume that the southern end of the lower crustal fault is controlled by the northwest-striking fault, the Wolf River fault (WRF), just north and east of Memphis (Cox, Van Arsdale, and Harris, 2001) that trends diagonally across the underlying western Reelfoot rift boundary and Crowley's Ridge (Fig. 6). The WRF appears to truncate the straight segment of the BCF and the Blytheville arch. The northern end of the deep-seated New Madrid fault may be controlled by the faults in the transitional area between the NMSZ and a more diffuse area of seismicity in the southern Illinois basin.
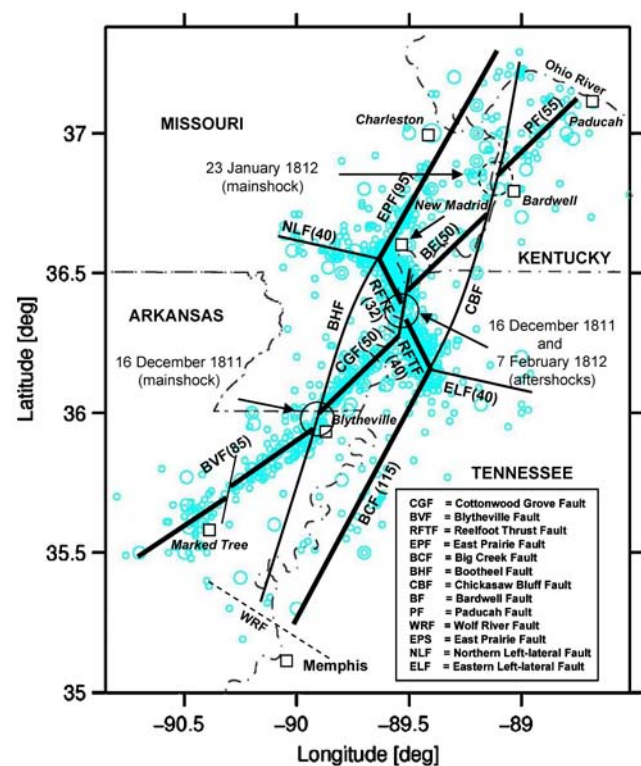
Figure 6. The potential rupture scenario for the 1811–1812 earthquake sequence. The conceptual NMSZ fault model developed in this study suggests that the subparallel faults in the upper crust are each divided into two segments (BHF/EPF and BCF/CBF). The fault model shows that the 1811–1812 earthquakes sequences occurred along the fault segments after the deep-seated fault transferred the stress to the brittle upper crust. The open circles with solid black lines represent the location of the 1811–1812 New Madrid earthquakes. The open circle with the dashed black line is the high stress concentration to generate the 1812 mainshock earthquake. The length of fault ruptures is estimated in kilometers. The color version of this figure is available only in the electronic edition.

Thus, the length of the deep-seated New Madrid fault in this conceptual model is estimated to be 240 km. The deep-seated fault movement creates a suite of subsidiary strike-slip structures within the overlying upper crust, which controls the shape of the NMSZ (Fig. 6). The proposed NMSZ model shows that the BHF/EPF and BCF/CBF are significant in shaping the geometry of the NMSZ. This model gives rise to a predictable pattern of surface deformation, which is in good agreement with the observed geometry and the specific trends related to modern seismicity in the NMSZ.

Segmented faults typically join together into a single fault at depth in intraplate regions (Segall and Pollard, 1980). The pattern of modern seismicity along the deep-seated New Madrid fault illustrates that the fault geometry in three dimensions may be as shown in Figure 7. This pattern of segmented left-stepping en echelon faults within the 15 km overburden material above the deep-seated fault is consistent with the pattern of seismicity and concepts of material failure in the NMSZ. We infer a direct relationship between the Blytheville arch and a major source zone in the NMSZ consistent with the conclusions of Crone (1998). The conceptual NMSZ model of faulting interprets the arch as a secondary structural feature that lies above a deep-seated fault zone along which the small earthquakes are occurring. Thus, the Blytheville arch is a flower structure formed by a lateral slip on a deep-seated fault zone.

The large earthquakes tend to occur close to fault intersections. In our estimates of fault rupture lengths, we used 50 km for the CGF and 85 km for BVF, which yields a total length of 134 km for the southern portion of the deep-seated New Madrid fault. This compares favorably with the 134 km length of the arch estimated using the reflection data (Crone, 1998) and the 125 km length of the model developed by Johnston and Schweig (1996). The north portion of the New Madrid fault consists of the 50 km long BF and the 55 km long PF, which yields a total length of ~105 km. Modern microearthquake data from the northeast NMSZ show an alignment of earthquakes that runs northeast from the southeast of New Madrid to north of Bardwell, Kentucky, and continues via the intersecting CBF and PF to ~10 km west-northwest of Paducah, Kentucky. The focal mechanism solutions for earthquakes in this area (Shumway, 2008) show that the fault pattern and stress regime are consistent with right-lateral slip along the EPF. Thus, the segmented BF and PF are predicted to have a right-lateral strike-slip component.

We believe that the segmented faults (BVF, CGF, BF, and PF) join together into a single fault at depth in the lower crust (Fig. 7). The relative movement of these segmented faults shows a series of en echelon Riedel *R* shear faults in the brittle upper crust. The conceptual model of deep-seated New Madrid fault developed in this study is consistent with the seismicity, geological features, elastic dislocation theory, and concepts of material failure under a stress field in the NMSZ (Segall and Pollard, 1980; Schweig and Ellis, 1994; Van Arsdale *et al.*, 1998). The two segmented faults proposed herein (BF and PF) on the northeast part of the
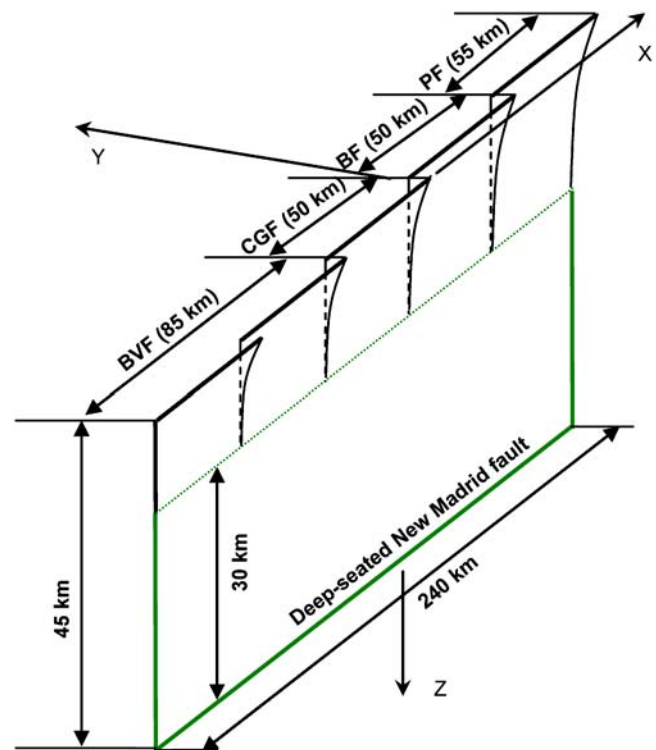
Figure 7. Three-dimensional model of deep-seated faulting in the NMSZ. The deep-seated New Madrid model is derived based on the elastic dislocation theory, the concepts of material failure under a stress field, the spatial pattern of modern seismicity, and on the fault geometry in the NMSZ. The segmented faults (BVF, CGF, BF, and PF) join together into a single fault at depth in the lower crust. The relative movement of these segmented faults shows a series of en echelon Riedel *R* shear faults in the brittle upper crust. BVF, Blytheville fault; CGF, Cottonwood Grove fault; BF, Bardwell fault; PF, Paducah fault. The color version of this figure is available only in the electronic edition.

deep-seated New Madrid fault might have been the sources of large earthquakes in the region. Intersection of the BF and PF segments with the CBF is possibly the location of the 23 January 1812 earthquake (Fig. 6).

Interpretation and Discussion

The three-dimensional NMSZ fault model developed in this study reflects a regional force couple leading to right-lateral strike-slip movement over a wide zone and the upward propagation of a deep-seated strike-slip fault to the surface and development of primary faults and subsidiary faults. Favorably oriented basement faults of the northeast-striking Reelfoot rift system and northwest-striking basement faults would accommodate this upward propagation.

The three-dimensional NMSZ fault model uses the intersections of the deep-seated faulting and the two subparallel faults (BHF/EPF and BCF/CBF) for the locations of the 1811 and 1812 earthquakes. The deep-seated New Madrid fault movement deforms the overlying upper crust that controls the geometry and the modern seismicity of the NMSZ.

Previous studies based on simple two-dimensional numerical models and rupture scenarios for the earthquake sequences (Gomberg, 1992; Mueller *et al.*, 2004) indicate that the 16 December 1811 and 7 February 1812 earthquakes of the four principal New Madrid earthquakes occurred along the two well-defined fault segments, the CGF and the RFTF, respectively. The northern end of the CGF continues as a linking fault on the RFTF, which is likely to be the location of the 7 February 1812 earthquake. The southern end of the CGF intersects with the BHF and is the location of the 16 December 1811 earthquake. The 16 December 1811 aftershock may have occurred on either of these faults. The location of the 23 January 1812 earthquake remains speculative. Although the earthquake in previous studies has been interpreted as a strike-slip rupture located along the EPF segment (Z3 in Fig. 1), Mueller *et al.* (2004) found this rupture scenario problematic and proposed a location at $-88.4°$ W, $36.95°$ N, 100 km northeast of the location near New Madrid in Figure 1.

To explore a new rupture scenario for the New Madrid earthquake sequence, we have developed a conceptual model of a deep-seated fault (Fig. 7), which is consistent with the seismicity, elastic dislocation theory, and concepts of material failure within the current stress field in the NMSZ. The NMSZ model geometry shows that the pattern and fault slip of modern seismicity and the types of faulting that occurred during the 1811–1812 New Madrid earthquakes can be derived from a deep-seated fault in the lower crust. A regional compressional stress field leads to the rotation of the principal stress directions and localized areas of enhanced stress near fault intersections. The December 1811 New Madrid earthquake is placed along the deep-seated fault segments from Blytheville to Little Prairie (BF and CGF segments). The deep-seated New Madrid fault continues as a linking fault called New Markham fault (Van Arsdale, 2000) to the BF and PF along two northeast-striking fault segments onto the BCF/CBF. The January 1812 New Madrid earthquake is likely to have been along the northeastern portion of the deep-seated New Madrid fault. Fault intersections control earthquake occurrence, earthquake sizes, and earthquake sequences by loading stresses on intersecting faults (Talwani, 1999). As shown in Figure 6, the 1811 and 1812 New Madrid mainshock earthquakes are located on intersecting faults. A combination of right-lateral movement on two subparallel *P* shear faults (BHF/EPF and BCF/CBF) with the right-lateral mainshock of the 1811 and 1812 earthquake loaded compressive stress onto the RFTF zone. The results of this loading suggest that the RFTF probably triggered the two aftershocks of the 1811 and 1812 earthquakes located on intersecting faults (Fig. 6). This interpretation is consistent with the numerical model of fault ruptures proposed by Mueller *et al.* (2004).

Modern seismicity in the NMSZ also fits the fault geometric model developed in this study (Fig. 6). For instance, the geological evidence indicates that the length of the RFTF consists of the ∼32 km long thrust fault from the intersection of the CGF and the RFTF to the west of New Madrid, and the ∼40 km long thrust fault from the CGF intersection to the

northeast of Dyersburg. Focal mechanism solutions for events along the fourth seismic zone (Z4) shown in Figure 1 indicate left-lateral slip on an ∼40 km long near-vertical plane, which is called NLF. The proposed NMSZ model of faulting predicts a possible ∼40 km long left-lateral strike-slip fault (ELF) near Dyersburg. Thus, we believe that there are two conjugate antithetic Riedel (R') shear faults (NLF and ELF) that branch from the ends of RFTF (Fig. 6). The reason is that the regional stress field (Fig. 4a–c) encourages right-lateral strike slip on the subparallel *P* shear faults (BHF/EPF and BCF/CBF) and left-lateral movement on the conjugate Riedel (R') shear faults. The buildup of stresses and tendency for rotation leads to localized compression at the intersection and combined with the thrust fault ruptures (RFTF) produces the pattern of modern seismicity in this area. These extensions and compressions are also the sources of the modern seismicity in the NMSZ.

The magnitude estimates of the 1811–1812 earthquakes vary by nearly an order of magnitude (Hough *et al.*, 2000; Mueller and Pujol, 2001). Assuming an inferred rupture area of $A = 240 \times 12$ km^2 by ignoring discontinuities for the 1811–1812 mainshock earthquakes in the NMSZ, the corresponding maximum expected magnitude would be equivalent to an **M** 7.5 earthquake with a standard deviation of 0.23 magnitude unit (Wells and Coppersmith, 1994). We assumed a nonseismogenic depth of 3 km in the NMSZ because the segmented faults do not reach the surface. Alternatively if a stress drop of ∼75 bars is assumed for the large earthquakes (e.g., 7 February 1812 event) corresponding to an average fault slip of ∼1.8 m (independent uplift measurement converted to fault slip [Merritts and Hesterberg, 1994]), then the cumulative seismic moment is $M_0 \approx 5.97 \times 10^{26}$ dyne cm and the corresponding moment magnitude would be equivalent to a **M** 7.2 earthquake. We assumed a rigidity of 3.5×10^{11} dyne/cm^2 (Turcotte and Schubert, 1982) for relatively stiff continental crust. Assuming a constant stress drop of ∼75 bars for the 1811 and 1812 New Madrid mainshock earthquakes, then the estimated seismic moment is $M_0 \approx 1.97 \times 10^{27}$ dyne cm, and the corresponding moment magnitude would be equivalent to an **M** 7.5 earthquake, which is consistent with the value estimated by fault size and earthquake magnitude. Our magnitude results are in good agreement with the magnitude estimated by Mueller *et al.* (2004) and inconsistent with the magnitude of the earthquake proposed by Johnston (1996), who suggested an **M** 8.0 ± 0.3, for the 1811–1812 large mainshock earthquakes.

Conclusions

In this study we have proposed a three-dimensional conceptual model of faulting to explain the occurrence of earthquakes in the NMSZ that is based on fault patterns of strike-slip systems. Our proposed deep-seated right-lateral strike-slip model gives rise to a predictable pattern of surface deformation that is in good agreement with observed

seismicity patterns in the NMSZ. Additionally, the model makes predictions that can be tested with improved data sets. For example, we predict an antithetic fault (ELF) in the Dyersburg, Tennessee, area. We have proposed two new segmented right-lateral strike-slip faults, BF and PF, based on surface expressions of deep-seated New Madrid faulting, and focal mechanisms in the northeast NMSZ.

Combination of seismic records with the proposed model provides the best opportunities for study of the long-term behavior of active faults in the NMSZ. Such knowledge of the long-term behavior of the NMSZ would provide a better understanding of seismic source zones to predict the next location of large earthquakes. Differences in the configurations between our model and previous NMSZ models could have significant effects on estimations of the seismic hazard at particular sites in the NMSZ.

On the basis of the proposed model in this study, the NMSZ coincides with a 240 km long deep-seated fault along the axis of Reelfoot rift and two subparallel P shear faults that play a significant role in the surface deformation, stress concentration, and the prediction of secondary fault systems in the brittle upper crust. Our results suggest that the four largest earthquakes of the 1811–1812 New Madrid sequence may have occurred along a single fault, intersecting two subparallel P shear faults. The NMSZ fault model developed in this study indicates that the displacement value of ~2 m during the 1811–1812 mainshock earthquakes is more plausible than the ~8 m of fault slip proposed by Johnston (1996). Thus, the estimates of maximum earthquake magnitudes in the area indicate a relatively lower value of $\mathbf{M}$ 7.5 on average for the 1811–1812 mainshock earthquakes instead of $\mathbf{M}$ 8.0.

The conceptual NMSZ fault model developed in this study has advantages over the many models that have been put forward in the literature during the past decade. The proposed model clarifies the pattern of modern seismicity, surface features, triggered slip on overlying faults, and the NMSZ earthquake sequence. The probabilistic seismic hazard models that represent uncertainty in the possible location of the NMSZ earthquake sequence are inconsistent with our model based on magnitude size and surface deformation associated with the 23 January 1812 earthquake. Although the previous probabilistic models (e.g., Petersen *et al.*, 2008) have been shown to relate directly to present-day seismicity or hypothetical faults, the large earthquakes may occur on known and unknown faults not characterized by frequent small seismic events. These active structures, which are unrecognizable through modern microearthquake data, may be the source of the next large earthquakes in the region. We suggest that the conceptual NMSZ model of faulting developed in this study be used as an alternative working model for defining locations of possible earthquake sequences, fault ruptures scenarios, earthquake magnitudes, and hence the future seismic hazard of the area.

It is possible to predict potential fault patterns at the ground surface, active deformation, and stress field in the NMSZ from the stresses produced by the en echelon strike-slip faults. The distribution of stress is markedly different in the region between two subparallel P shear faults. To illustrate this contrast, a quantitative model of NMSZ deformation based on the present model needs to be tested in a future study using a three-dimensional numerical method.

Data and Resources

All data used in this paper came from published sources listed in the references.

Acknowledgments

References

Bakun, W. H., and M. G. Hopper (2004). Historical seismic activity in the central United States, *Seism. Res. Lett.* **75,** 564–574.

Braile, L. W., W. J. Hinze, G. R. Lidiak, and E. G. Sexton (1986). Tectonic development of the New Madrid rift complex, Mississippi embayment, North America, *Tectonophysics* **131,** 1–21.

Chiu, J. M., A. C. Johnston, and Y. T. Yang (1992). Imaging the active faults of the central New Madrid seismic zone using PANDA array data, *Seism. Res. Lett.* **63,** 375–393.

Chiu, S. C., J. M. Chiu, and A. C. Johnston (1997). Seismicity of the southeastern margin of Reelfoot rift, central United States, *Seism. Res. Lett.* **68,** 785–796.

Cox, R. T., and R. B. Van Arsdale (1997). Hotspot origin of the Mississippi embayment and its possible impact on contemporary seismicity, *Eng. Geol.* **46,** 5–12.

Cox, R. T., and R. B. Van Arsdale (2002). The Mississippi embayment, North America: A first order continental structure generated by the Cretaceous superplume mantle event, *J. Geodyn.* **34,** 163–176.

Cox, R. T., R. B. Van Arsdale, and J. B. Harris (2001). Identification of possible Quaternary deformation in the northeastern Mississippi embayment using quantitative geomorphic analysis of drainage-basin asymmetry, *Bull. Geol. Soc. Am.* **113,** 615–624.

Cox, R. T., R. B. Van Arsdale, J. B. Harris, and D. Larsen (2001). Neotectonics of the southeastern Reelfoot rift zone margin, central United States, and implications for regional strain accommodation, *Geology* **29,** 419–422.

Crone, A. J. (1998). Defining the southwestern end of the Blytheville arch, northeastern Arkansas: Delimiting a seismic source zone in the New Madrid region, *Seism. Res. Lett.* **69,** 350–358.

Csontos, R., and R. Van Arsdale (2008). New Madrid seismic fault geometry, *Geol. Soc. Am.* **4,** 802–813.

Csontos, R., R. Van Arsdale, R. Cox, and B. Waldron (2008). Reelfoot rift and its impact on Quaternary deformation in the central Mississippi River valley, *Geol. Soc. Am.* **4,** 145–158.

Eaton, D. W., and A. Frederiksen (2007). Seismic evidence for convection-driven motion of the North American plate, *Nature* **446,** 428–431.

Ellis, W. L. (1994). Summary and discussion of crustal stress data in the region of the New Madrid seismic zone, *U.S. Geol. Surv. Profess. Pap. 1538-A-C*, B1–B13.

Gan, W., and W. H. Prescott (2001). Crustal deformation rates in central and eastern U.S. inferred from GPS, *Geophys. Res. Lett.* **28,** 3733–3736.

Gomberg, J. (1992). Tectonic deformation in the New Madrid seismic zone: Inferences from boundary-element modeling, *Seism. Res. Lett.* **63,** 407–426.

Gomberg, J., and M. Ellis (1994). Topography and tectonic of the central New Madrid seismic zone: Results of numerical experiments using

a three-dimensional boundary element program, *J. Geophy. Res.* **99,** 20,299–20,310.

Guccione, M. J., R. Marple, and W. J. Autin (2005). Evidence for Holocene displacements on the Bootheel fault (lineament) in southeastern Missouri: Seismotectonic implications for the New Madrid region, *Bull. Geol. Soc. Am.* **117,** 319–333.

Hamilton, R. M., and A. C. Johnston (1990). Tecumseh's prophecy: Preparing for the next New Madrid earthquake, *U.S. Geol. Surv. Circular* **1066,** 30 pp.

Hamilton, R. M., and F. A. McKeown (1988). Structure of the Blytheville arch in the New Madrid seismic zone, *Seism. Res. Lett.* **59,** 117–121.

Hamilton, R. M., and M. D. Zoback (1982). Tectonic features of the New Madrid seismic zone from seismic-reflection profiles, in *Investigations of the New Madrid, Missouri, Earthquake Region*, F. A. Mckeown and L. C. Pakiser (Editors), *U.S. Geol. Surv. Profess. Pap. 1236*, 55–82.

Herrmann, R. B. (1979). Surface wave focal mechanisms for eastern North America earthquakes with tectonic implication, *J. Geophys. Res.* **84,** 3543–3552.

Herrmann, R. B., and J. A. Canas (1978). Focal mechanism studies in the New Madrid seismic zone, *Bull. Seismol. Soc. Am.* **68,** 1095–1102.

Hildenbrand, T. G., M. F. Kane, and J. D. Hendricks (1982). Magnetic basement in the upper Mississippi embayment region—A preliminary report, in *Investigations of the New Madrid, Missouri, Earthquake Region*, F. A. Mckeown and L. C. Pakiser (Editors), *U.S. Geol. Surv. Profess. Pap. 1236*, 39–53.

Hildenbrand, T. G., J. G. Rosenbaum, and R. L. Reynolds (1992). High-resolution aeromagnetic study of the New Madrid seismic zone: A preliminary report, *Seism. Res. Lett.* **63,** 209–221.

Himes, L., W. Stauder, and R. B. Herrmann (1988). Indication of active faults in the New Madrid seismic zone from precise locations of hypocenters, *Seism. Res. Lett.* **59,** 123–132.

Hough, S. E., and S. Martin (2002). Magnitude estimates of two large aftershocks of the 16 December 1811 New Madrid earthquake, *Bull. Seismol. Soc. Am.* **92,** 3259–3268.

Hough, S. E., J. G. Armbruster, and L. Seeber (2000). On the modified Mercalli intensities and magnitudes of 1811–1812 New Madrid earthquakes, *J. Geophys. Res.* **105,** 23,839–23,864.

Howe, J. R. (1985). Tectonics, sedimentation, and hydrocarbon potential of the Reelfoot Aulocogen, *Master's Thesis*, University of Oklahoma, 109 pp.

Jibson, R. W., and D. K. Keefer (1992). Analysis of the seismic origin of a landslide in the New Madrid seismic zone, *Seism. Res. Lett.* **63,** 427–437.

Johnson, G. (2008). Using earthquake focal mechanisms to investigate seismotectonics in New Madrid seismic zone, *Master's Thesis*, University of Memphis.

Johnston, A. C. (1996). Seismic moment assessment of earthquakes in stable continental regions-III, New Madrid 1811–1812, Charleston 1886, and Lisbon 1755, *Geophys. J. Int.* **126,** 314–344.

Johnston, A. C., and E. S. Schweig (1996). The enigma of the New Madrid earthquake of 1811–1812, *Ann. Rev. Earth Planet. Sci.* **24,** 339–384.

Kelson, K. I., G. D. Simpson, R. B. Van Arsdale, J. B. Harris, C. C. Haraden, and W. R. Lettis (1996). Multiple Late Holocene earthquakes along the Reelfoot fault, central New Madrid seismic zone, *J. Geophys. Res.* **101,** 6151–6170.

Kenner, S. J., and P. Segall (2000). A mechanical model for intraplate earthquakes: Application to the New Madrid seismic zone, *Science* **289,** 2329–2332.

Liu, L., and M. D. Zoback (1997). Lithospheric strength and intraplate seismicity in the New Madrid seismic zone, *Tectonics* **16,** 585–595.

Mandl, G. (1988). The mechanics of tectonic faulting; models and basic concepts, in *Developments in Structural Geology*, H. J. Zwart (Editor), Elsevier, Amsterdam, 408 pp.

McKeown, F. A., R. M. Hamilton, S. F. Diehl, and E. E. Glick (1990). Diapiric origin of the Blytheville and Pascola arches in the Reelfoot rift, east-central United States: Relation to New Madrid seismicity, *Geology* **18,** 1158–1162.

Merritts, D., and T. Hesterberg (1994). Stream networks and long-term surface uplift in the New Madrid seismic zone, *Science* **265,** 1081–1084.

Mooney, W. D., M. C. Andrews, A. Ginzburg, D. A. Peters, and R. M. Hamilton (1983). Crustal structure of the northern Mississippi embayment and a comparison with other rift zones, *Tectonophysics* **94,** 327–348.

Mueller, K., and J. Pujol (2001). Three-dimensional geometry of the Reelfoot blind thrust: Implications for moment release and earthquake magnitude in the New Madrid seismic zone, *Bull. Seismol. Soc. Am.* **91,** 1563–1573.

Mueller, K., S. E. Hough, and R. Bilham (2004). Analysing the 1811–1812 New Madrid earthquakes with recent instrumentally recorded aftershocks, *Nature* **429,** 284–288.

Nelson, W. J., F. B. Denny, J. A. Devera, L. R. Follmer, and J. M. Masters (1997). Tertiary and Quaternary tectonic faulting in southernmost Illinois, *Eng. Geol.* **46,** 235–258.

Newman, A., S. Stein, J. Weber, J. Engeln, A. Mao, and T. Dixon (1999). Slow deformation and lower seismic hazard at the New Madrid seismic zone, *Science* **284,** 619–621.

Nuttli, O. W. (1973). The Mississippi valley earthquakes of 1811 and 1812, intensities, ground motion, and magnitudes, *Bull. Seismol. Soc. Am.* **63,** 227–248.

Petersen, M. D., A. D. Frankel, S. D. Harmsen, C. S. Mueller, K. M. Haller, R. L. Wheeler, R. L. Wesson, Y. Zeng, O. S. Boyd, D. M. Perkins, N. Luco, E. H. Field, C. J. Wills, and K. S. Rukstales (2008). Documentation for the 2008 update of the United States national seismic hazard maps, *U.S. Geol. Surv. Open-File Rept. 2008-1128*, 61 pp.

Ramsey, J. G. (1980). Shear zone geometry: A review, *J. Struct. Geol.* **2,** 83–92.

Rodgers, D. A. (1980). Analysis of pull-apart basin development produced by en-echelon strike slip faults, in *Sedimentation in Oblique-Slip Mobile Zones*, Ballance, P. F., and H. G. Reading (Editors), Special Publications of the International Association of Sedimentologists, Vol. 4, 27–41.

Russ, D. P. (1982). Style and significance of surface deformation in the vicinity of New Madrid, Missouri, in *Investigations of the New Madrid, Missouri, Earthquake Region*, F. A. McKeown and L. C. Parkiser (Editors), *U. S. Geol. Surv. Profess. Pap. 1236*, 95–114.

Scholz, C. H. (1990). *The Mechanics of Earthquakes and Faulting*, Cambridge U Press, Cambridge, 439 pp.

Schweig, E. S., and M. A. Ellis (1994). Reconciling short recurrence interval with minor deformation in the New Madrid seismic zone, *Science* **264,** 1308–1311.

Schweig, E. S., and R. T. Marple (1991). The Bootheel lineament: A possible cosesimic fault of the great New Madrid earthquakes, *Geology* **19,** 1025–1028.

Schweig, E. S., F. S. Shen, L. R. Kanter, E. A. Luzietti, R. B. Van Arsdale, K. M. Shedlock, and K. W. King (1992). Shallow seismic reflection survey of the Bootheel lineament area, southeastern Missouri, *Seism. Res. Lett.* **63,** 285–295.

Seeber, L., and J. G. Armbruster (1991). The NCEER-91 earthquake catalog: Improved intensity-based magnitudes and recurrence relations for U.S. earthquakes east of New Madrid, National Center for Earthquake Engineering Research, NCEER-91-0021.

Segall, P., and D. D. Pollard (1980). Mechanics of discontinuous faults, *J. Geophys. Res.* **85,** 4337–4350.

Shumway, A. M. (2008). Focal mechanisms in the northeast New Madrid seismic zone, *Seism. Res. Lett.* **79,** 469–477.

Smalley, R., M. A. Ellis, J. Paul, and R. B. Van Arsdale (2005). Space geodetic evidence for rapid strain rates in the New Madrid seismic zone of central USA, *Nature* **435,** 1088–1090.

Stauder, W. (1982). Present-day seismicity and identification of active faults in the New Madrid seismic zone, in *Investigations of the New Madrid, Missouri, Earthquake Region*, F. A. McKeown and L. C. Parkiser, *U.S. Geol. Surv. Profess. Pap. 1236*, 21–30.

Sykes, L. R. (1978). Intraplate seismicity, reactivation of pre-existing zones of weakness, alkaline magmatism, and other tectonism postdating continental fragmentation, *Rev. Geophys.* **16,** 621–688.

Talwani, P. (1999). Fault geometry and earthquakes in continental interiors, *Tectonophysics* **303,** 371–379.

Tchalenko, J. S. (1970). Similarities between shear zones of different magnitudes, *Bull. Geol. Soc. Am.* **81,** 1625–1640.

Tchalenko, J. S., and N. N. Ambraseys (1970). Structural analysis of the Dash-e-Bayaz (Iran) earthquake fractures, *Bull. Geol. Soc. Am.* **81,** 41–60.

Turcotte, D. L., and G. Schubert (1982). *Geodynamics: Applications of Continuum Physics to Geophysical Problems*, John Wiley and Sons, New York.

Van Arsdale, R. B. (2000). Displacement history and slip rate on the Reelfoot fault of the New Madrid seismic zone, *Eng. Geol.* **55,** 219–226.

Van Arsdale, R. B., R. T. Cox, A. C. Johnston, W. J. Stephenson, and J. K. Odum (1999). Southeastern extension of the Reelfoot fault, *Seism. Res. Lett.* **70,** 352–363.

Van Arsdale, R. B., K. I. Kelson, and C. H. Lumsden (1995). Northern extension of the Tennessee Reelfoot scarp into Kentucky and Missouri, *Seism. Res. Lett.* **66,** 57–62.

Van Arsdale, R. B., J. Purser, W. J. Stephenson, and J. K. Odum (1998). Faulting along the southern margin of Reelfoot Lake, Tennessee, *Bull. Seismol. Soc. Am.* **88,** 131–139.

Wells, D. L., and K. J. Coppersmith (1994). Updated empirical relationships between magnitude, rupture length, rupture area and surface displacement, *Bull. Seismol. Soc. Am.* **84,** 972–1002.

Wilcox, R. E., T. P. Harding, and D. R. Seely (1973). Basic wrench tectonics, *Bull. Am. Assoc. Petrol. Geol.* **57,** 74–96.

Zoback, M. D., and M. L. Zoback (1981). State of stress and intraplate earthquakes in the U.S., *Science* **213,** 96–104.

Zoback, M. D., R. M. Hamilton, A. J. Crone, D. P. Russ, F. A. McKeown, and S. R. Brockman (1980). Recurrent intraplate tectonism in the New Madrid seismic zone, *Science* **209,** 971–976.

Zoback, M. L. (1992). Stress field constrains on intraplate seismicity in eastern North America, *J. Geophys. Res.* **97,** no. B8, 11,761–11,782.

Geotechnical & Hydraulic Engineering Services
Bechtel Corporation
Frederick, Maryland 21703
   (B.T.)

Department of Civil Engineering
The University of Memphis
Memphis, Tennessee 38152
   (S.P.)

Department of Earth Sciences
The University of Memphis
Memphis, Tennessee 38152
   (R.T.C.)